Journal of Applied Polymer Science

Effects of different ionizable groups on the thermal properties of waterborne polyurethanes used in bulletproof composites

Yan Li,[1,2] Jian Zheng,[1] Yunjun Luo,[1] Hong Zhou,[2] Qingchun Wang[2]

[1]School of Materials Science and Engineering, Beijing Institute of Technology, Beijing 100081, People's Republic of China
[2]Quartermaster Research Institute, General Logistics Department, Beijing 100088, People's Republic of China
Correspondence to: Y. J. Luo (E-mail: yjluo@bit.edu.cn)

ABSTRACT: The thermal stability of the resin matrix is an important factor affecting the safety performance of fiber-reinforced bulletproof composites (FRBCs) during their service period. In this study, two kinds of waterborne polyurethanes based on polyester diol (PEDL218) and isophorone diisocyanate were synthesized; these were used as the matrix of para-aramid FRBCs. Their thermal stability and thermal decomposition behaviors in a nitrogen atmosphere were studied by dynamic thermogravimetric analysis techniques. The kinetic parameters, including the activation energy (E) and pre-exponential factor (A), were calculated by the Flynn–Wall–Ozawa, Kissinger–Akahira–Sunose, Kissinger, and Šatava–Šesták methods. The results show that the cationic waterborne polyurethane with quaternary ammonium groups has better thermal stability than the anionic waterborne polyurethane with carboxylate groups. Their nonisothermal decomposition mechanisms were studied, and the kinetic parameters were also calculated; this will offer theoretical reference for the manufacturing and application of FRBCs based on waterborne polyurethane. © 2015 Wiley Periodicals, Inc. J. Appl. Polym. Sci. **2015**, *132*, 42374.

KEYWORDS: composites; degradation; kinetics; resins; thermogravimetric analysis (TGA)

Received 4 February 2015; accepted 13 April 2015
DOI: 10.1002/app.42374

INTRODUCTION

Waterborne polyurethane (WPU) is a kind of polymer dispersed in water. It has the advantages of good properties, for example, a light smell, no pollution, and energy savings;[1] this is in accordance with environmental guidelines. In recent years, WPU has been used for the preparation of unidirectional fiber-reinforced bulletproof composites (FRBCs), a kind of composite widely used in the applications demanding ballistic protection, as a substitute for traditional solvent-based resins (vinyl ester resins, phenolic resins, and styrene–isoprene–styrene block copolymer). After a dipping and hot-pressing process, WPU is combined with *para*-aramid fibers to become strip composite laminates. Then, these materials (unidirectional FRBCs) can be processed into a variety of products according to different ballistic protection applications.

The ballistic mechanism of the FRBCs during high-speed impact involves many factors, including the properties of fiber and resin, the interfacial interaction of fiber and matrix, the arrangement of fibers in the composite and the processing conditions.[2] The resin matrix can significantly influence the performance of the bulletproof composites, although the amount of matrix is small (typically in the range 10–20 wt %). Under impact, the resins are involved in energy transfer and absorption and keep the fibers in the distribution beneficial to absorb energy.[3] As well know, the motion of bullets in a gun chamber can produce lots of heat because of friction, so there may be a high temperature around the projectiles. Therefore, the thermal stability is another important property of the resin matrix; it can affect the safety of bulletproof composites in a service period. The study and evaluation of the thermal properties are always key research fields related to bulletproof equipment.[4–6] For aramid/WPU bulletproof composites, the aramid fiber has excellent thermal stability, but that of the WPU is much lower. Therefore, WPU is a main factor affecting the thermal stability of composites. Obviously, the properties of materials are closely related to their structure. According to the charge characteristics of hydrophilic groups, WPU can be divided into cationic type (quaternary ammonium groups), anionic type (carboxylate or sulfonate groups), and nonionic type [water-soluble poly(ethylene glycol) groups or hydrophilic copolyether groups].[7] Previous studies have shown that the sorts and concentration of the hydrophilic ionic groups can greatly affect the physical and chemical properties of WPU, such as the hardness, modulus, tensile strength, elongation at break, glass-transition temperature, and particle size of the polyurethane dispersion.[8–10] However, the influence of ionizable groups on the thermal stability and thermal decomposition kinetics of WPU has not been

studied. Indeed, more attention should be paid to these problems in the processing and use of bulletproof composites. When these ionic groups were used to adjust the material properties, we also hope to understand their effects on the thermal stability of the materials, which is important for the manufacture and application of bulletproof composites.

Thermogravimetric analysis (TGA) techniques have been widespread used for the study of the thermal stability and the thermal decomposition of polymers. A number of researchers have studied the thermal decomposition behaviors of polyurethane foam,[11,12] elastomer,[13–15] adhesive,[16] and coating.[17] The kinetic parameters and models of the reactions were calculated by different experimental and calculation methods based on TGA techniques. For instance, Lefebvre *et al.*[11] investigated the modeling of the mass losses of rigid polyurethane foam under linear heating rates (β) in an inert atmosphere with the invariant kinetic parameters method. Hyoe *et al.*[12] used the Flynn–Wall–Ozawa (FWO) method to calculate the thermal decomposition activation energy (E) of biobased polyurethane composite foams filled with inorganic fillers and predicted the durability of the materials through the dynamic parameters.

In this study, two kinds of WPUs based on polyester diol (PEDL218) and isophorone diisocyanate (IPDI) were synthesized and used as the resin matrixes for para-aramid FRBCs. Next, a comparative study of the thermal stability of these WPUs with different ionizable groups (the quaternary ammonium groups and the carboxylate groups) was made with dynamic TGA techniques. Their kinetic parameters and models of the thermal decomposition were evaluated by the FWO, Kissinger–Akahira–Sunose (KAS), Kissinger, and Šatava–Šesták methods. The results of this research will offer theoretical reference for the manufacturing and application of FRBCs based on WPU.

EXPERIMENTAL

Materials

Polyester diol [PEDL218; number-average molecular weight (M_n) = 2000] was purchased from Yantai Huada Chemical Co., Ltd. 1,4-Butanediol (BDO) was purchased from Shanxi Sanwei Co., Ltd. Dimethylol propionic acid (DMPA) was purchased from Anqing Zhongda Chemical Co., Ltd. IPDI was purchased from Germany Bayer Co., Ltd. Acetone was purchased from Beijing Yanshan Chemical Co., Ltd. Triethylamine (TEA) was purchased from Shijiazhuang Shijilongxin Co., Ltd. *N*-Methyl diethanolamine (MDEA) was purchased from Changzhou Yuping Chemical Co., Ltd. Glacial acetic acid was purchased from Liaoning Shuangding Chemical Co., Ltd., and dimethyl sulfate was purchased from Nantong Dalun Chemical Co., Ltd.

Synthetic Method

AWPU was synthesized according to the modified acetone process.[1] A 1000-mL, four-necked round-bottom flask, equipped with a stirrer and thermometer, was added with 200 g of polyester diol (PEDL218, M_n=2000) and 9 g of BDO. The mixture was stirred and heated to 110°C to dehydrate it *in vacuo* for 2 h. Then, the reaction temperature dropped to 80°C in the presence of nitrogen, and 11.2 g of DMPA, 85.7 g of IPDI, and 50 g of acetone were added to the flask. After 6 h of stirring, the temperature dropped to 60°C. The mixture and 8.4 g of TEA were put into the emulsification tank and stirred. Then, 650 g of distilled water was added to the mixture. The product (AWPU) was filtered and obtained. In the preparation of the AWPU, polyester diol (PEDL218) was used as the soft segment, and IPDI was extended with BDO and DMPA as the hard segments. DMPA was used as the ionic center, and TEA was used as a neutralizer.

CWPU was prepared with the same raw materials used in the preparation of the AWPU as the soft segments, but its hard segments were made up of IPDI, BDO, and MDEA. To a 1000-mL, four-necked, round-bottomed flask equipped with a stirrer and a thermometer were added 200 g of polyester diol (PEDL218, M_n = 2000), 9 g of BDO, and 10 g of MDEA. The mixture was stirred and heated to 110°C to dehydrate *in vacuo* for 2 h. Then, the reaction temperature was decreased to 80°C in the presence of nitrogen, and 85.7 g of IPDI and 50 g of acetone were added to the flask. After 6 h of stirring, the temperature was decreased to 60°C. An amount of 10 g of dimethyl sulfate was added to the flask, and the reaction mixture was refluxed for 0.5 h. The mixture and 55 g of glacial acetic acid were put into the emulsification tank and stirred. Then, 650 g of distilled water was added to the mixture. The product (CWPU) was filtered and obtained. In the preparation of the CWPU, MDEA was used as the ionic center, and glacial acetic acid was used as a neutralizer.

Finally, the resin films of the two samples were prepared by the placement of 30 mL of WPU onto a polytetrafluoroethylene plate, followed by drying at room temperature for 1 week. The final films were then dried at 60°C *in vacuo* for 24 h.

Fourier Transform Infrared (FTIR) Spectroscopy

FTIR spectroscopy was performed on the WPU films in attenuated total reflectance mode with a Nicolet iN10 spectrometer. The spectra were recorded at a 4-cm^{-1} resolution from 500 to 4000 cm^{-1}.

^{1}H-NMR Spectra

A Bruker ARX-400 NMR spectrometer was used to obtain the ^{1}H-NMR spectra with dimethyl sulfoxide as the solvent.

TGA

TGA of all samples was performed with a TA Instruments Q50 instrument. The samples (3–5 mg) were heated from ambient temperature to 500°C at various βs: 10, 20, 30, and 40 K/min. A high-purity nitrogen stream was continuously passed into a furnace at a flow rate of 60 mL/min.

Kinetic Methods

According to nonisothermal kinetic theory, the kinetic equation of the solid matter thermal decomposition can be expressed as follows:[18]

$$\frac{d\alpha}{dT} = \frac{A}{\beta}\exp\left(-\frac{E}{RT}\right)f(\alpha) \quad (1)$$

where α is the conversion of the reaction (%), β is the heating rate (K/min), A is the pre-exponential factor (min^{-1}), E is the apparent activation energy (J/mol), T is the absolute temperature (K), and R is the gas constant [8.314 J $(mol{\cdot}K)^{-1}$], $f(\alpha)$ is

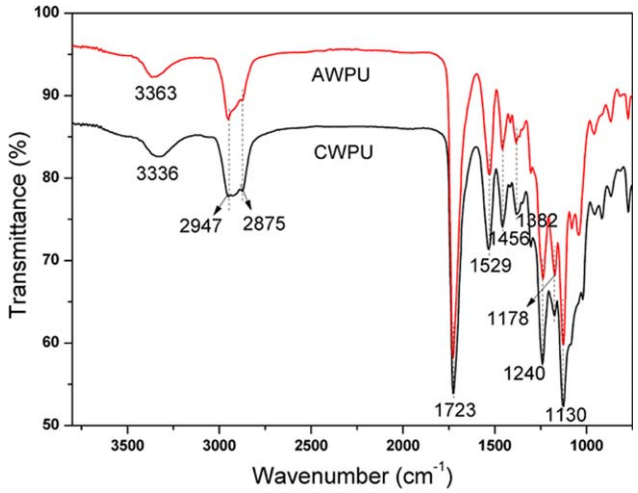

Figure 1. FTIR spectra curves of CWPU and AWPU. [Color figure can be viewed in the online issue, which is available at wileyonlinelibrary.com.]

a mathematical model function of kinetics which depends on the reaction type and reaction mechanism.

KAS Method. The KAS method[19,20] is an integral isoconversional linear method; the equation is expressed as follows:

$$\ln\left(\frac{\beta}{T^2}\right) = \ln\frac{AE}{g(\alpha)R} - \frac{E}{RT} \tag{2}$$

where $g(\alpha)$ is the integral form of the reciprocal of $f(\alpha)$ and can be expressed as shown in eq. (3), which is the reaction model and depends on the reaction mechanism:

$$g(\alpha) = \int_0^{\alpha} d\alpha/f(\alpha) \tag{3}$$

From eq. (2), plots of $\ln(\beta/T^2)$ versus $1/T$ were made, and E was calculated from the slopes of these lines at different αs.

FWO Method. The FWO method[21] is another common integral method, which can determine E only through given values of α. The integral form of the FWO method is represented by eq. (4).

$$\lg\beta = \lg\frac{AE}{g(\alpha)R} - 2.315 - 0.4567\frac{E}{RT} \tag{4}$$

Because the value of $\log\{AE/[Rg(\alpha)]\}$ is approximately a constant when the values of α are the same at the different βs, the plot $\log\ \beta$ versus $1/T$ is approximately linear. Thus, with the plotting of $\log\ \beta$ against $1/T$ at certain percentage α, the slope $(-0.4567E/R)$ leads to E.

Kissinger Method. The Kissinger method is a common differential method used to study the thermal decomposition mechanism; it can determine E and A. The Kissinger method[19,22,23] is expressed by eq. (5):

$$\ln\frac{\beta}{T_p^2} = \ln\frac{AR}{E} - \frac{E}{RT_p} \tag{5}$$

where T_p is the peak temperature of the differential thermogravimetry (DTG) curve (K). By plotting $\ln(\beta/T_p^{\ 2})$ versus $1/T_p$, the activation energy calculated by the Kissinger–Akahira–Sunose method (E), and the pre-exponential factor calculated by the Kissinger–Akahira–Sunose method (A) can be calculated on the basis of the slope $(-E/R)$ and intercept $[\ln(AR/E)]$, respectively.

Šatava–Šesták Method. The Šatava–Šesták method is used to fit the nonisothermal decomposition mechanism of the solid materials. The expression form of this method[24] is given by eq. (6).

$$\lg g(\alpha) = \lg\frac{A_S E_S}{R\beta} - 2.315 - 0.4567\frac{E_S}{RT} \tag{6}$$

where A_s is the pre-exponential factor calculated by the Šatava–Šesták method (s^{-1}), E_s is the apparent activation energy calculated by the Šatava–Šesták method (J/mol), and g(α) comes from 1 of 30 forms of an integral formula in the literature.[25,26]

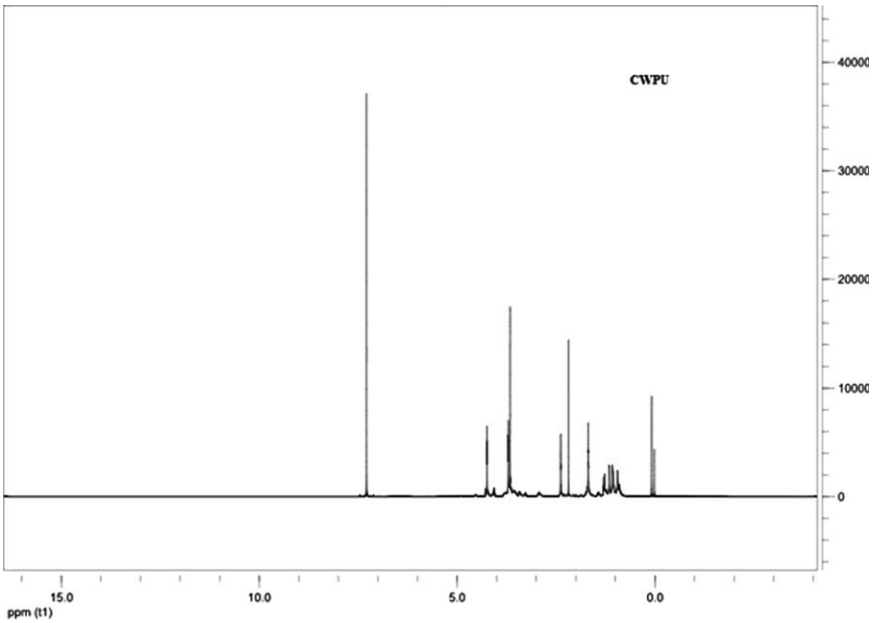

Figure 2. ^{1}H-NMR spectra of CWPU.

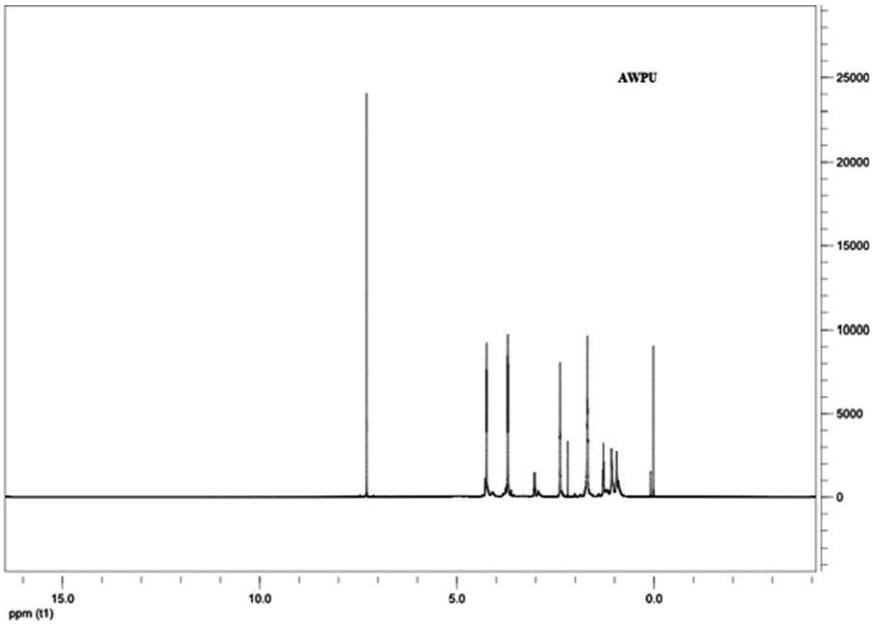

Figure 3. ^{1}H-NMR spectra of AWPU.

For fixed β, the values of E_s and A_s can be obtained with eq. (6) at any selected g(α). Therefore, we could obtain 30 sets of values for E_s and ln A_s, and the mechanism functions of the thermal decomposition reactions could be found through these data. Generally, the $g(\alpha)$ values are kept as long the following condition is met: $0 < E_s < 400$ kJ/mol. So, we needed to compare the values of E_s and ln A_s with E_o and ln A_k, respectively, where E_o comes from the FWO method and ln A_k comes from the Kissinger method. If the results meet with $|(E_o - E_s)/E_o| \leq 0.1$ and $|(\ln A_s - \ln A_k)/\ln A_s| \leq 0.4$, the corresponding $g(\alpha)$ will be an integral form of the most probable mechanism function of the reaction.

RESULTS AND DISCUSSION

FTIR Analysis

The FTIR spectra of the CWPU and AWPU are revealed in Figure 1. There were three characteristic absorbance peaks of polyurethane in the curves: the 3336 and 3363-cm^{-1} peaks due to N—H stretching vibrations, the peak at 1723 cm^{-1} due to the C═O stretching vibrations of the urethane carbonyl group, and the peak at 1529 cm^{-1} due to the N—H bending vibrations.[27,28] Moreover, the other absorption peaks in the curves were as follows: those at 2947 and 2875 cm^{-1} due to C—H stretching vibrations, those at 1456 and 1382 cm^{-1} due to CH_2 and CH_3 deformation vibrations, and those at 1130 cm^{-1}, 1178, and 1240-cm^{-1} peaks due to the C—O vibrations of polyester. This indicates that the two substances synthetized in this research were all polyester polyurethane and their main functional groups were highly similar. According to the shifting of the N—H stretching vibrations, we observed that CWPU had a higher degree of hydrogen bonding than AWPU.[29] Furthermore, no absorption peak of the NCO group (2270 cm^{-1}) was observed in these samples; this indicated that the NCO groups of the prepolymer reacted completely with the chain extenders during the chain-extension step.

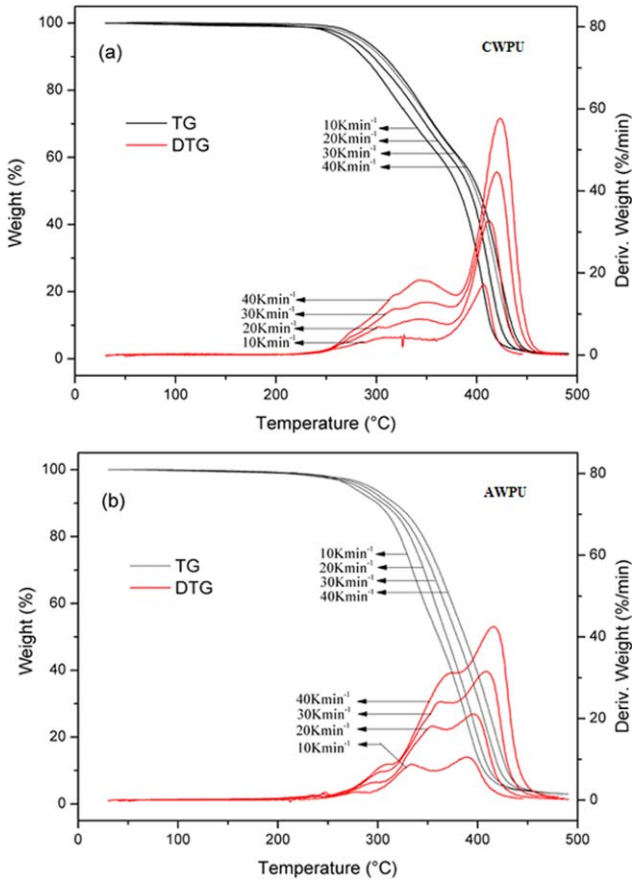

Figure 4. TG and DTG curves of (a) CWPU and (b) AWPU under a nitrogen atmosphere at four βs (10, 20, 30, and 40 K/min). [Color figure can be viewed in the online issue, which is available at wileyonlinelibrary.com.]

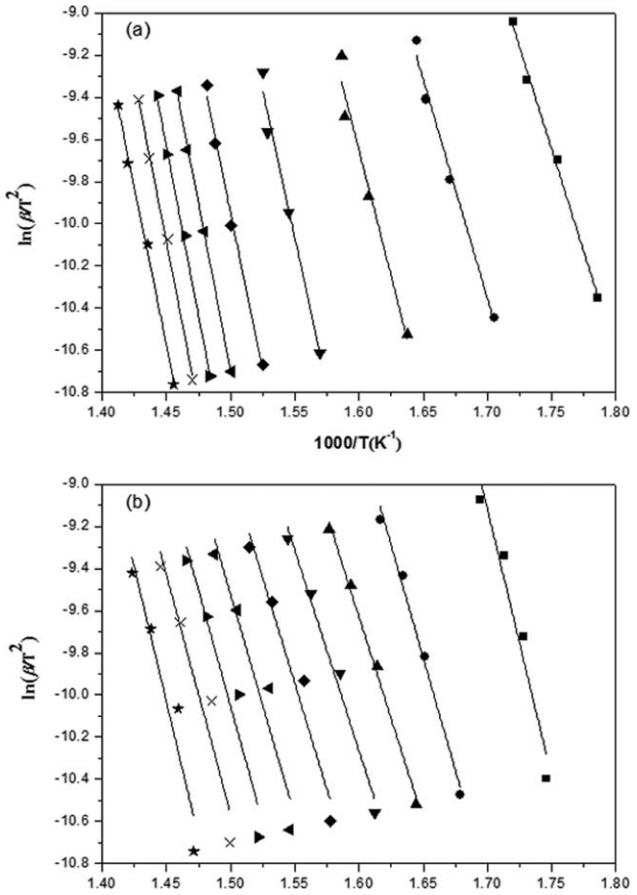

Figure 5. Plots of the KAS method for the thermal decomposition *E* of (a) CWPU and (b) AWPU. The αs of the reaction were (■) 0.1, (•) 0.2, (▲) 0.3, (▼) 0.4, (◆) 0.5 (◀) 0.6, (▶) 0.7, (×) 0.8, and (★) 0.9.

^{1}H-NMR Analysis

The NMR results of CWPU and AWPU are shown in Figures 2 and 3.

^{1}H-NMR (CWPU, δ, ppm): 2.38 (s, 3H), 3.66 (t, 4H), 3.71 (s, 3H) and 4.24 (t, 4H).

The peak at 2.38 ppm corresponded to the protons of N—CH_3. The peak at 3.66 ppm corresponded to the protons of N—CH_2. The peak at 3.71 ppm corresponded to the protons of O—CH_3. The peak at 4.24 ppm corresponded to the protons of O—CH_2—C.

^{1}H-NMR (AWPU, δ, ppm): 1.28 (s, 3H), 1.68 (t, 3 × 3H), 3.71 (q, 3 × 2H) and 4.25 (s, 4H).

The peak at 1.28 ppm corresponded to the protons of C—CH_3. The peak at 1.68 ppm corresponded to the protons of 3 × C—CH_3. The peak at 3.71 ppm corresponded to the protons of 3 × N—CH_2. The peak at 4.25 ppm corresponded to the protons of O—CH_2—C. The results of ^{1}H-NMR already show that AWPU and CWPU were successfully synthesized.

TGA

Thermogravimetry (TG) and DTG curves at different βs (10, 20, 30, and 40 K/min) of the CWPU and AWPU are shown in Figure 4(a,b). All of the TG curves exhibited a sharp mass loss from 100 to 500°C; these were accompanied by a peak in the weight loss rate in the DTG curves. The curves under different βs had an approximate shape, and the peaks shifted to high temperature with increasing β. Looking at the details of the TG curves, we found that the 50% mass loss for AWPU and CWPU occurred at 361 and 383°C, respectively. This indicated that CWPU had a better thermal stability than AWPU. This may have been attributed to their different hard-segment structures and interactions between the hard and soft segments.

The DTG curves of CWPU and AWPU [Figure 4(a,b)] showed obviously that there were two major steps of mass loss. With the DTG curves at 10 K/min as an example, the first stage of the CWPU decomposition occurred in the range 267–368°C with a mass loss of 5–40%. Differently, AWPU occurred in the range 274–361°C with a mass loss of 5–50%. The C—O bond of urethane groups on the polymer backbone were broken and induced the generation of isocyanate and polyol; this further decomposed into amines, olefins, and CO_2.[30] In the second stage, the decomposition of CWPU occurred in the range 368–450°C with a mass loss of 40–95%. For the AWPU, it was 361–450°C with a 50–97% mass loss.

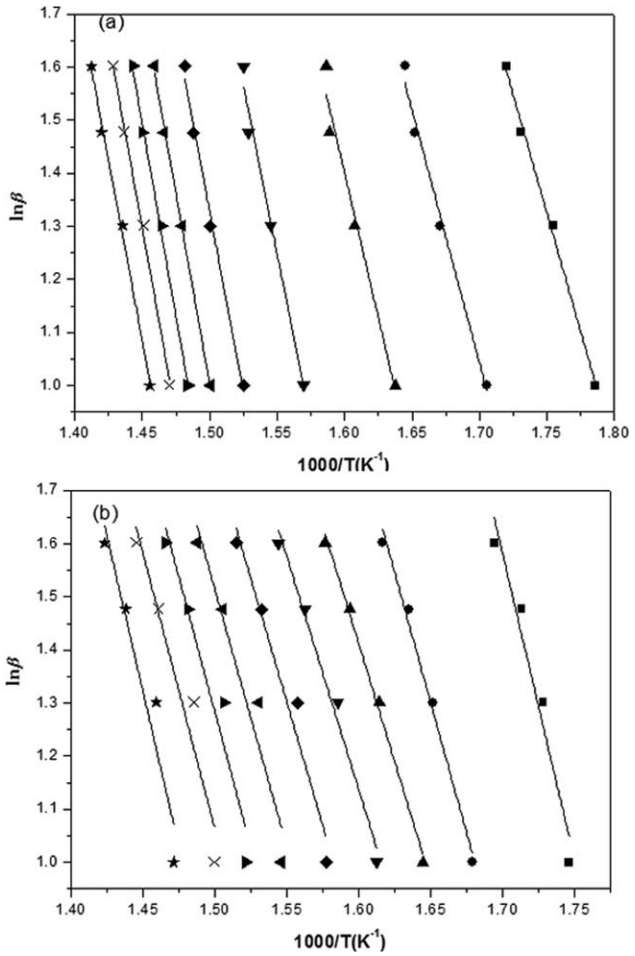

Figure 6. Plots of the FWO method for the thermal decomposition *E* of (a) CWPU and (b) AWPU. The αs of the reaction were (■) 0.1, (•) 0.2, (▲) 0.3, (▼) 0.4, (◆) 0.5 (◀) 0.6, (▶) 0.7, (×) 0.8, and (★) 0.9.

Table I. E Values of CWPU and AWPU Obtained with the KAS and FWO Methods

	Stage I[a]				Stage II[b]			
	KAS method		FWO method		KAS method		FWO method	
Sample	E (kJ/mol)[c]	R^2	E (kJ/mol)	R^2	E (kJ/mol)	R^2	E (kJ/mol)	R^2
CWPU	191.31	0.9768	191.55	0.9790	253.41	0.9909	251.67	0.9916
AWPU	176.92	0.9702	177.89	0.9731	180.77	0.9163	182.39	0.9252

[a] CWPU, $\alpha = 0$–0.4; AWPU, $\alpha = 0.4$–0.9.
[b] CWPU, $\alpha = 0$–0.5; AWPU, $\alpha = 0.5$–0.9.
[c] Relative uncertainty (u_r) = 0.02.

Nonisothermal Kinetic Studies

The kinetics of nonisothermal decomposition for CWPU and AWPU were investigated with the KAS, FWO, Kissinger, and Šatava–Šesták methods. In these works, the αs were set to specified values from 0.1 to 0.9. According to eqs. (2) and (4), the plots of $\ln(\beta/T^2)$ versus $1000/T$ (KAS) and $\ln \beta$ versus $1000/T$ (FWO) corresponding to different αs were obtained. As shown in Figures 5 and 6, a series of approximate parallel lines were obtained by the linear fitting method. The left-to-right lines in the graphs corresponded to α values of 0.9–0.1. E was calculated from the slopes of the lines at different αs.

The kinetic parameters calculated by KAS and FWO are given in Table I, and the relationship between E and α is shown in Figure 7. We found from Figure 7 that E of CWPU and AWPU varied throughout the decomposition process. The E values of CWPU quickly increased from 162.6 to 265.3 kJ/mol (FWO) with increasing α from 0.1 to 0.7 and then turn into a downward trend. On the contrary, the E values of AWPU decreased first and then increased slowly until the sample almost completely decomposed. This indicated that the thermal decomposition mechanism of CWPU and AWPU were completely different, although they had a similar structure. In the majority of thermal decomposition processes, the E values of CWPU were obviously higher than that of AWPU. Additionally, as shown in Figure 7 and Table I, we found that the E values calculated by the KAS method were in good agreement with the results of the FWO method.

According to eq. (5), the plots of $\ln(\beta/T_p^2)$ versus $1000/T_p$ were obtained (Figure 8), where T_p is the temperature at peak of the DTG curve for different βs. E and $\ln A$ were calculated on the basis of the slope ($-E/R$) and intercept [$\ln(AR/E)$], respectively. The calculated results are summarized in Table II. The results show that the correlation coefficients (R^2s) were greater than 0.97 for the Kissinger method. However, there was a significant

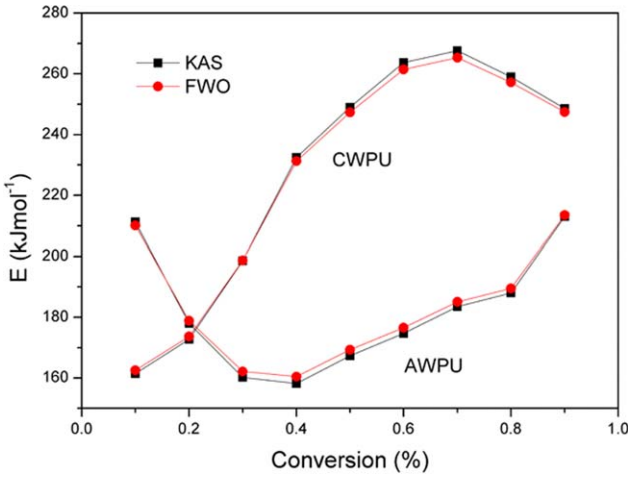

Figure 7. E of CWPU and AWPU at different αs. [Color figure can be viewed in the online issue, which is available at wileyonlinelibrary.com.]

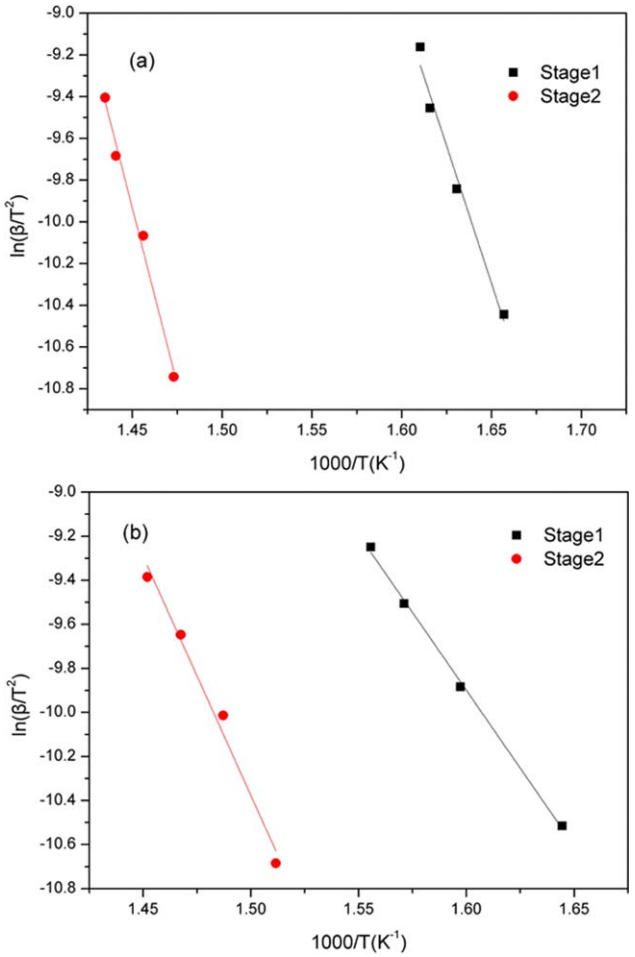

Figure 8. Plots of the Kissinger method for thermal decomposition E and A of (a) CWPU and (b) AWPU. [Color figure can be viewed in the online issue, which is available at wileyonlinelibrary.com.]

Table II. Values of E and ln A of the Thermal Decomposition of CWPU and AWPU Calculated with the Kissinger Method

	Stage I			Stage II		
Sample	E (kJ/mol)[a]	ln A (min^{-1})	R^2	E (kJ/mol)	ln A (min^{-1})	R^2
CWPU	219.11	36.46	0.9741	280.78	42.55	0.9976
AWPU	117.66	15.37	0.9848	180.44	25.25	0.9787

[a] Relative uncertainty (u_r) is 0.02.

deviation for the E values (Tables I and II) of AWPU in the first stages. This was attributed to the divergence of the calculating methods.[31]

The Šatava–Šesták method allowed us to compute E_s and ln A_s and model the thermal decomposition of the materials. In this study, the values of E_s and ln A_s for the different αs and βs were calculated by any selected g(α), according to eq. (6). The results, 30 sets of the values of E_s and ln A_s, are listed in Table III. The values of E_s and ln A_s were compared with the value of activation energy calculated by the Flynn–Wall–Ozawa method (E_o)

Table III. Values of E_s and ln A_s of the Thermal Decomposition of CWPU and AWPU Calculated with the Šatava–Šesták Method

	CWPU						AWPU					
	Stage I			Stage II			Stage I			Stage II		
No.	E_s (kJ/mol)[a]	ln A_s (min^{-1})	R^2	E_s (kJ/mol)[a]	ln A_s (min^{-1})	R^2	E_s (kJ/mol)[a]	ln A_s (min^{-1})	R^2	E_s (kJ/mol)[a]	ln A_s (min^{-1})	R^2
1	101.61	10.27	0.9624	136.55	12.93	0.9962	154.55	14.90	0.9885	89.38	9.43	0.9934
2	106.07	10.40	0.9669	170.16	15.42	0.9908	100.22	9.87	0.9742	170.16	15.42	0.9908
3	107.66	9.90	0.9684	185.85	16.07	0.9869	102.05	9.39	0.9759	185.85	16.07	0.9869
4	110.85	10.21	0.9713	218.38	18.77	0.9778	105.73	9.74	0.9790	218.38	18.77	0.9778
5	27.71	4.80	0.9713	54.60	6.72	0.9778	26.43	4.70	0.9790	54.60	6.72	0.9778
6	27.12	4.83	0.9692	48.69	6.35	0.9843	25.75	4.73	0.9768	48.69	6.35	0.9843
7	95.40	8.70	0.9572	116.20	10.22	0.9970	88.65	8.10	0.9633	116.20	10.22	0.9970
8	89.48	8.12	0.9513	97.94	8.65	0.9976	82.46	7.50	0.9568	97.94	8.65	0.9976
9	57.86	7.20	0.9751	136.26	13.32	0.9625	55.69	7.01	0.9831	136.26	13.32	0.9625
10	38.58	5.80	0.9751	90.84	9.76	0.9625	37.13	5.68	0.9831	90.84	9.76	0.9625
11	28.93	5.14	0.9751	68.13	8.01	0.9625	27.84	5.05	0.9831	68.13	8.01	0.9625
12	19.29	4.53	0.9751	45.42	6.32	0.9625	18.56	4.47	0.9831	45.42	6.32	0.9625
13	14.47	4.26	0.9751	34.06	5.51	0.9625	13.92	4.22	0.9831	34.06	5.51	0.9625
14	115.73	11.63	0.9751	272.51	24.24	0.9625	111.38	11.24	0.9831	272.51	24.24	0.9625
15	173.59	16.19	0.9751	408.77	35.28	0.9625	167.06	15.59	0.9831	408.77	35.28	0.9625
16	231.45	20.79	0.9751	545.02	46.38	0.9625	222.75	19.99	0.9831	545.02	46.38	0.9625
17	54.24	6.57	0.9692	97.38	9.85	0.9843	51.50	6.33	0.9768	97.38	9.85	0.9843
18	55.43	6.50	0.9713	109.19	10.64	0.9778	52.86	6.28	0.9790	109.19	10.64	0.9778
19	56.03	6.43	0.9723	115.52	11.03	0.9743	53.56	6.22	0.9801	115.52	11.03	0.9743
20	44.49	6.27	0.9465	32.70	5.34	0.9807	40.56	5.94	0.9494	32.70	5.34	0.9807
21	38.89	5.93	0.9274	15.60	4.30	0.9279	34.56	5.57	0.9243	15.60	4.30	0.9279
22	33.96	5.61	0.9055	7.50	3.96	0.8633	29.47	5.25	0.8950	7.50	3.96	0.8633
23	50.80	6.55	0.9624	68.27	7.81	0.9962	47.58	6.27	0.9691	68.27	7.81	0.9962
24	76.21	8.38	0.9624	102.41	10.34	0.9962	71.38	7.95	0.9691	102.41	10.34	0.9962
25	25.40	4.84	0.9624	34.14	5.41	0.9962	23.79	4.72	0.9691	34.14	5.41	0.9962
26	16.93	4.35	0.9624	22.76	4.68	0.9962	15.86	4.27	0.9691	22.76	4.68	0.9962
27	12.70	4.14	0.9624	17.07	4.36	0.9962	11.90	4.09	0.9691	17.07	4.36	0.9962
28	14.87	4.56	0.9852	176.35	16.98	0.8512	17.31	4.72	0.9578	176.35	16.98	0.8512
29	65.67	7.93	0.9847	244.63	22.25	0.9131	64.90	7.87	0.9915	244.63	22.25	0.9131
30	7.43	4.11	0.9852	88.18	9.78	0.8512	8.66	4.16	0.9578	88.18	9.78	0.8512

[a] Relative uncertainty (u_r) = 0.02.

and the value of ln A_k obtained by the Kissinger method, respectively. The results show that in the first stage, the decomposition reaction of the CWPU was consistent with the mechanism of nucleation and growth.[26] The form of the integral equations for the mechanism function was $g(\alpha) = [-\ln (1 - \alpha)]^3$. However, AWPU had no appropriate functional form consistent with the mechanism of thermal decomposition. Moreover, the values of E_s and ln A_s were 173.59 kJ/mol and 16.19/min for CWPU and 167.06 kJ/mol and 15.59/min for AWPU, respectively. In the second stage, the thermal decomposition mechanism for CWPU was consistent with the chemical reactions, The form of the integral equations for the mechanism function was $g(\alpha) = (1 - \alpha)^{-1} - 1$. However, the mechanism for AWPU was consistent with three-dimensional cylindrical symmetric diffusion,[26] the form of the integral equations for the mechanism function was $g(\alpha) = (1 - 2/3\alpha) - (1 - \alpha)^{2/3}$. So, the values of E_s and ln A_s of the CWPU in the second stage were regarded as 244.63 kJ/mol and 22.25/min, respectively; those of AWPU were 185.85 kJ/mol and 16.07/min, respectively.

CONCLUSIONS

In summary, two kinds of WPUs with different charge properties were synthesized to study the influence of a hydrophilic chain extender on the thermal decomposition behaviors of WPU in a nitrogen atmosphere. The thermal stability was investigated by dynamic TGA techniques. The results of the experiment indicate that the decomposition reaction of CWPU and AWPU could be divided into two stages. CWPU had better thermal stability than AWPU. This observation was confirmed in the literature[32] by the investigation of the dissociation energies of CH—H (452 kJ/mol), CH_2—H (473 kJ/mol), C—N (770 kJ/mol), and *OC*═O (532 kJ/mol). The CH—H and CH_2—H bonds probably generated simultaneous scission under high temperatures. Next were *OC*═O and C—N bonds. In the structure of CWPU, the C—N bond was the main chain of the polymer, and the C—N bond was in the side chain of AWPU. The degradation of CWPU needed more energy. Kinetic parameters were calculated with the FWO, KAS, Kissinger, and Šatava–Šesták methods. The most probable kinetic function [$g(\alpha)$] of the thermal decomposition was established by the Šatava–Šesták method. The results show that the decomposition reaction of CWPU in the first stage was consistent with the mechanism of nucleation and growth. The form of the integral equations for the mechanism function was $g(\alpha) = [-\ln(1 - \alpha)]^3$. However, AWPU did not have an appropriate functional form consistent with the mechanism of thermal decomposition. Moreover, the values of E_s and ln A_s were 173.59 kJ/mol and 16.19/min, respectively, for CWPU and 167.06 kJ/mol and 15.59/min, respectively, for AWPU. In the second stage, the decomposition reaction of CWPU was consistent with the chemical reactions, and the form of the integral equations was $g(\alpha) = (1 - \alpha)^{-1} - 1$. The mechanism for AWPU was consistent with three-dimensional cylindrical symmetric diffusion, and the form of the integral equations was $g(\alpha) = (1 - 2/3\alpha) - (1 - \alpha)^{2/3}$. The values of E_s and ln A_s of the CWPU in the second stage were 244.63 kJ/mol and 22.25/min, respectively. For AWPU, the values of E_s and ln A_s were 185.85 kJ/mol and 16.07/min, respectively. These results were helpful to the manufacturing and application of FRBCs based on WPU. In the design of the resin matrix for bulletproof material or in the hot processing of FRBCs, information about the thermal stability and thermal degradation of WPU is needed.

ACKNOWLEDGMENTS

This work was supported by the National High Technology Research and Development Program of China (863 Program; contract grant number 2012AA03A209).

REFERENCES

1. Sardon, H.; Irusta, L.; Fernández-Berridi, M. J.; Luna, J.; Lansalot, M.; Bourgeat-Lami, E. *J. Appl. Polym. Sci.* **2011**, *120*, 2054.
2. Moryea, S. S.; Hinea, P. J.; Ducketta, R. A.; Carrb, D. J.; Warda, I. M. *Compos. A* **1999**, *30*, 649.
3. Gopinath, G.; Zheng, J. Q.; Batra, R. C. *Compos. Struct.* **2012**, *94*, 2690.
4. Akay, M.; Mun, K. S. A.; Stanley, A. *Compos. Sci. Technol.* **1997**, *57*, 565.
5. Halvorsen, A.; Khojn, A. S.; Mahinfalah, M. *Appl. Compos. Mater.* **2006**, *13*, 369.
6. Vivas, V.; Souto, M. B. G. *Sci. Eng. Compos. Mater.* **2007**, *14*, 1.
7. Mohammad, M. R.; Kim, H. D. *J. Appl. Polym. Sci.* **2006**, *102*, 5684.
8. Nanda, A. K.; Wicks, D. A.; Madbouly, S. A. *J. Appl. Polym. Sci.* **2005**, *98*, 2514.
9. Lee, S. K.; Kim, B. K. *J. Colloid Interface Sci.* **2009**, *336*, 208.
10. Tsai, H. C.; Hong, P. D.; Yen, M. S. *Text. Res. J.* **2007**, *77*, 710.
11. Lefebvre, J.; Duquesne, S.; Mamleev, V.; Le Bras, M.; Delobel, R. *Polym. Adv. Technol.* **2003**, *14*, 796.
12. Hyoe, H.; Noriko, T.; Hiroshi, M.; Shigeo, H.; Tatsuko, H. *J. Thermochim. Acta* **2005**, *431*, 155.
13. Lv, Y.; Luo, Y. J.; Guo, K.; Wang, X. P. *J. Solid Rocket Technol.* **2010**, *3*, 315.
14. Fambri, L.; Pegoretti, A.; Gavazza, C.; Penati, A. *J. Appl. Polym. Sci.* **2001**, *81*, 1216.
15. Yuan, K. J.; Jiang, Z.; Li, S. F.; Zhou, Y. *Chin. J. Appl. Chem.* **2005**, *22*, 861.
16. Li, A. L.; Xiong, J. P.; Zuo, Y.; Wang, C. Z. *Acta Phys. Chim. Sin.* **2007**, *23*, 1622.
17. Ni, B. L.; Yang, L. T.; Wang, C. S.; Wang, L. Y.; Finlow, D. E. *J. Therm. Anal. Calorim.* **2010**, *100*, 239.
18. Vyazovkin, S.; Burnham, A. K.; Criado, J. M.; Pérez-Maqueda, L. A.; Popescu, C.; Sbirrazzuoli, N. *Thermochim. Acta* **2011**, *520*, 1.
19. Kissinger, H. E. *J. Anal. Chem.* **1957**, *29*, 1702.
20. Akahira, T.; Sunose, T. *Res. Rep. Chiba Inst. Technol. (Sci. Technol.).* **1971**, *16*, 22.
21. Ozawa, T. *Bull. Chem. Soc. Jpn.* **1965**, *38*, 1881.

22. Rotaru, A.; Kropidlowska, A.; Anca, M. *J. Therm. Anal. Calorim.* **2008**, *92*, 233.
23. Kissinger, H. E. *J. Res. Nat. Bur. Stand.* **1956**, *57*, 217.
24. Šatava, F.; Šesták, J. *J. Therm. Anal. Calorim.* **1975**, *8*, 477.
25. Huang, M. X.; Lv, S. C.; Zhou, C. R. *Thermochim. Acta* **2013**, *552*, 60.
26. Hu, R. Z.; Shi, Q. Z. Thermal Dynamics; Science: Beijing, **2008**; p 62.
27. Rehab, A.; Salahuddin, N. *Mater. Sci. Eng.* **2005**, *399*, 368.
28. Pollack, S. K.; Shen, D. Y.; Hsu, S. L.; Wang, Q.; Stidham, H. D. *Macromolecules* **1988**, *22*, 270.
29. Wang, C. B.; Cooper, S. L. *Macromolecules* **1983**, *16*, 775.
30. Yoshitake, N.; Furukawa, M. *J. Anal. Appl. Pyrolysis* **1995**, *33*, 269.
31. Shao, X. Z.; Wang, L. S.; Li, M. Y.; Jia, D. M. *Thermochim. Acta* **2012**, *547*, 70.
32. Speight, J. G. Lange's Handbook of Chemistry, 16th ed.; McGraw-Hill: New York, **2010**; p 2467.